

# Adsorption of Linear and Spherical DNA Oligonucleotides onto Microplastics

Mohamad Zandieh, Kshiti Patel and Juewen Liu\*

Department of Chemistry, Waterloo Institute for Nanotechnology, University of Waterloo

Waterloo, Ontario, N2L 3G1, Canada

Email: liujw@uwaterloo.ca

## Abstract

Microplastic pollution of water and food chains can endanger human health. It has been reported that environmental DNA can be carried by microplastics and spread into ecosystem. To better comprehend the interactions between microplastics and DNA, we herein investigated the adsorption of DNA oligonucleotides on a few important microplastics. The microplastics were prepared using common plastic objects made of polyethylene (PE), polypropylene (PP), polystyrene (PS), polyvinyl chloride (PVC), composite of PS/PVC, and polyethylene terephthalate (PET). The effect of environmentally abundant metal ions such as  $\text{Na}^+$ ,  $\text{Mg}^{2+}$  and  $\text{Ca}^{2+}$  on the adsorption was also studied. Amongst the microplastics, PET and PS had the highest efficiency for the adsorption of linear DNA, likely due to the interactions provided by their aromatic rings. The study of DNA desorption from PET revealed the important role of hydrogen bonding and metal-mediated adsorption, while van der Waals force and hydrophobic interactions were also involved in the adsorption mechanism. The adsorption of spherical DNA (SNA) made of a high density of DNA coated on gold nanoparticles (AuNPs) was also studied, where the adsorption affinity order was found to be  $\text{PET} > \text{PS/PVC} > \text{PS}$ . Moreover, a tighter DNA adsorption was achieved in the presence of  $\text{Ca}^{2+}$  and  $\text{Mg}^{2+}$  compared to  $\text{Na}^+$ .

## Introduction

Plastic materials are extremely prevalent due to their low price, light weight, versatility, and durability. Over 300 million tons of plastics are produced annually.<sup>1</sup> However, they do not degrade easily in the environment. Therefore, plastic wastes contaminate the soil, sea, fresh water, and food chains.<sup>2-4</sup> When plastic materials are broken into tiny pieces (<1 mm) in the environment *via* mechanical force, chemical transformations, or microbiological degradation, microplastics are formed.<sup>5</sup> Due to a high surface-to-volume ratio of microplastics, a wide range of invasive marine microorganisms can adsorb onto microplastics and spread into the ecosystem.<sup>6-8</sup> It is estimated that annually a minimum of 39000-52000 microplastic particles are consumed by each individual,<sup>9</sup> posing a serious threat to human health potentially leading to particle toxicity, disruption of the immune system, and cancer in long term.<sup>10-11</sup> The most extensively detected microplastics in freshwaters are composed of polyethylene (PE), polypropylene (PP), polystyrene (PS), polyvinyl chloride (PVC), and polyethylene terephthalate (PET).<sup>12</sup>

Studying the interactions between DNA and microplastics particularly is important for a few reasons.<sup>13-17</sup> On one hand, DNA is an important biopolymer, and biological DNA can be carried by microplastics in the environment. For example, extraction and sequencing of environmental DNA from marine microplastics have been investigated widely.<sup>18-21</sup> Moreover, adsorption of DNA onto PP, PS and polydimethylsiloxane (PDMS) have been reported.<sup>22-24</sup> Investigation of the adsorption of DNA oligonucleotides onto materials and surfaces can provide useful information regarding their interaction mechanism. On the other hand, DNA oligonucleotides might serve as a probe to detect and study microplastics. DNA aptamers have been selected against various inorganic and polymeric surfaces. Selecting aptamers for microplastics can be important for their extraction and detection. Before performing aptamer selections, it is important to understand nonspecific adsorption of DNA. If nonspecific adsorption is too strong, then it is difficult to obtain specific aptamers.<sup>25</sup> Besides single-stranded linear DNA, adsorption of spherical nucleic acids (SNA) may provide additional insights. SNA refers to a nanoparticle core (e.g. AuNP) functionalized with a high density of DNA oligonucleotides.<sup>26-29</sup> Previous works showed that SNA can adsorb onto surfaces with much higher affinity than linear DNA of the same sequence due to polyvalent interactions amplifying weak individual interactions

of a linear DNA.<sup>30-32</sup> The adsorption mechanism of SNA can also be different from linear DNA due to the confined conformation of the DNA.<sup>33</sup>

In this work, we investigated the interaction of linear and spherical DNA oligonucleotides with a few most common microplastics, and we pay particular attention to the effect of metal ions that are abundant in the environment such as  $\text{Na}^+$ ,  $\text{Mg}^{2+}$  and  $\text{Ca}^{2+}$ .<sup>34</sup> We observed that PET, PS/PVC and PS showed the highest affinity for DNA adsorption due to their more favorable surface functional groups, and divalent metal ions can promote efficient DNA adsorption.

## Materials and Methods

**Chemicals.** The 21-mer DNA (5'-AAA AAA AAA CCC AGG TTC TCT-3') and this DNA with different modifications (3'-FAM, or 5'-SH, or dual labeled 5'-SH and 3'-FAM) were purchased from Integrated DNA Technologies (IDT, Coralville, IA, USA). Metal chloride salts, ethylenediaminetetraacetic acid (EDTA), Tween 80, sodium polyphosphate (25-mer), and potassium cyanide (KCN) were from Sigma-Aldrich. 4-(2-Hydroxyethyl) piperazine-1-ethanesulfonic acid (HEPES), urea, and adenosine were obtained from Mandel Scientific (Guelph, ON, Canada) Citrate-capped AuNPs (13 nm) were synthesized based on the literature,<sup>35</sup> and the concentration of stock AuNPs was calculated to be  $\sim 10$  nM using the extinction coefficient of  $2.7 \times 10^8 \text{ M}^{-1} \text{ cm}^{-1}$  at 520 nm. Milli-Q water was used for the preparation of all the buffers and solutions.

**Instrumentation.** The Raman spectra of solid plastic samples were collected using a spectrometer (DeltaNu, Advantage 785) with a 785 nm laser and a 10 s integration time. The morphology of the microplastics was visualized under a Nikon Eclipse Ti-S inverted microscope, and the transmission electron microscopy (TEM) images were taken using a Phillips CM10 100 kV microscope. The  $\zeta$ -potentials of microplastics were measured using a dynamic light scattering (DLS) instrument (Zetasizer Nano 90, Malvern). In a typical experiment, the microplastics (final concentration of  $\sim 50 \mu\text{g/mL}$ ) were dispersed in 1 mL buffer (10 mM HEPES, pH 7.6), and the temperature was controlled at 25 °C.

**Preparation of Microplastics.** Six commonly used plastic objects were collected (Figure 1, insets) including a cylindrical plastic container (PE), a laboratory centrifuge tube (PP), a plastic

fork or spoon (PS), a plastic sheet (PVC), a hand-sanitizer dispenser container (composite of PS/PVC), and a water bottle (PET). The composing material of the plastic objects was identified using Raman spectroscopy.<sup>36-37</sup> Then, the plastics were cut into small pieces and washed with ethanol in a sonication bath for 2 min to remove the organic residues on the surface. Finally, using a stainless steel kitchen grater, the plastics were shredded into microplastics *via* mechanical force and were dispersed in Milli-Q water at a concentration of 2 mg/mL. Due to the size of the microplastics, and depending on their density, they either settled down to the bottom or float on top of the aqueous suspensions. The samples were used for further studies within two days after the preparation to minimize the possible effect of aging.

**Preparation of SNA.** The freezing-directed method was used to prepare SNA.<sup>38</sup> In this method, a final concentration of 3  $\mu$ M 5'-SH-DNA was mixed with 10 nM AuNPs and placed in a freezer (-20°C) for 3 h. After thawing at room temperature, the SNAs were centrifuged (14000 rpm, 15 min) at 15°C and washed 3 times with water. To measure the density of attached DNA, a dual labeled 5'-SH and 3'-FAM-DNA was used to prepare the SNA. The AuNPs core was then dissolved by adding KCN (a final of 10 mM). Finally, using a fluorescence intensity *vs.* DNA concentration standard curve, the number of DNA attached on each AuNPs was calculated.

**Adsorption of Linear DNA.** Typically, 10 nM FAM-DNA was incubated with  $\sim$ 50  $\mu$ g/mL of microplastics in the presence of different metal ions in a buffer (10 mM HEPES, pH 7.6). To avoid precipitation of microplastic particles, the samples were gently agitated during the incubation. After 1 h, the samples were centrifuged (1000 rpm, 2 min), and the fluorescence intensity of supernatants was measured to back-calculate the adsorbed DNA.

**Adsorption of SNA.** In a typical experiment, 1.58 nM SNA (total of  $\sim$ 200 nM DNA) was incubated with  $\sim$ 150  $\mu$ g/mL of microplastics in the presence of different metal ions in a buffer (10 mM HEPES, pH 7.6). To avoid precipitation of microplastic particles, the samples were gently agitated during the reaction. After 4 h, the samples were centrifuged (1000 rpm, 2 min), and the UV-vis absorbance of the supernatants were used to back-calculate the adsorbed SNA. The DNA and SNA concentration used was the minimum concentration at which a decent signal can be achieved. The concentration of microplastics also was optimized to ensure that the surface was in excess and was not a limiting factor to adsorb the DNA or SNA.

**DNA Desorption Studies.** To investigate the desorption of linear DNA, first, 10 nM FAM-DNA was adsorbed on PET in the presence of 200 mM Na<sup>+</sup>, 2 mM Mg<sup>2+</sup>, or 2 mM Ca<sup>2+</sup> for 1 h. The pre-adsorption experiments for this section were designed in a way to ensure that 100% of the DNA or SNA were adsorbed prior to desorption studies. Then, 4 M urea, 10 mM EDTA, 5 mM adenosine, 0.2 mM polyphosphate (25-mer, total phosphate concentration: 5 mM), or 0.25% Tween 80 was mixed with the pre-adsorbed DNA in the same buffer for 1 h. For the SNA desorption studies, first, 1.58 nM SNA (total of ~200 nM DNA) was adsorbed on the microplastics in the presence of 4 mM Mg<sup>2+</sup>, or 2 mM Ca<sup>2+</sup> overnight. Then, 4 M urea, or 10 mM EDTA was mixed with the pre-adsorbed SNA in the same buffer for 1 h. Finally, the supernatants of the samples were collected after centrifugation (1000 rpm, 2 min), and the desorbed DNA/SNA was quantified according to the fluorescence/absorbance enhancement.

## Results and Discussion

### Microplastics Preparation and Characterization

To best mimic microplastics in the environment, instead of using commercially available standard polymer microspheres, we prepared our microplastics samples *via* mechanical shredding of some commonly used plastic items such as water bottles and culinary utensils (insets of Figure 1). Using Raman spectroscopy, six types of plastic materials were identified and used for further studies including: PE, PP, PS, PVC, composite of PS/PVC, and PET (Figure 1). For example, the sample in Figure 1E had a strong peak at 1001 cm<sup>-1</sup>, which is the characteristic peak of aromatic ring from its PS component.<sup>39</sup> The location of the major characteristic peaks and the corresponding vibrational modes are summarized in Tables S1-5.

After shredding the plastics (Figure S1), the obtained microplastics were observed under a microscope (Figure 2). The morphology of the microplastics was irregular including a combination of fragments, fibers, and foams.<sup>40</sup> Although the particle size distribution was broad for each sample, on average, PE and PP had the largest particles and PET had the smallest. This was likely due to the difference between the manufacturing and mechanical properties of the plastic materials. Nevertheless, all samples fulfilled the size requirement (<1 mm) to be defined as microplastics.<sup>5</sup>

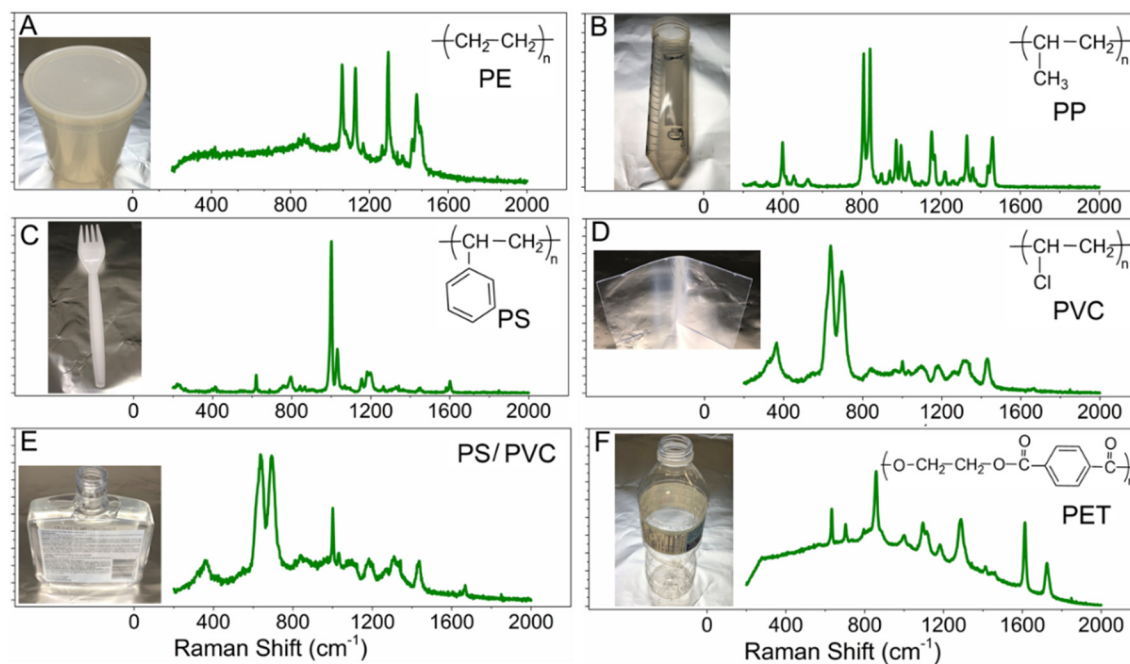


**Figure 1.** Photographs , Raman spectra and molecular structures of the plastic materials used in this work including: (A) PE, (B) PP, (C) PS, (D) PVC, (E) composite of PS/PVC, and (F) PET.

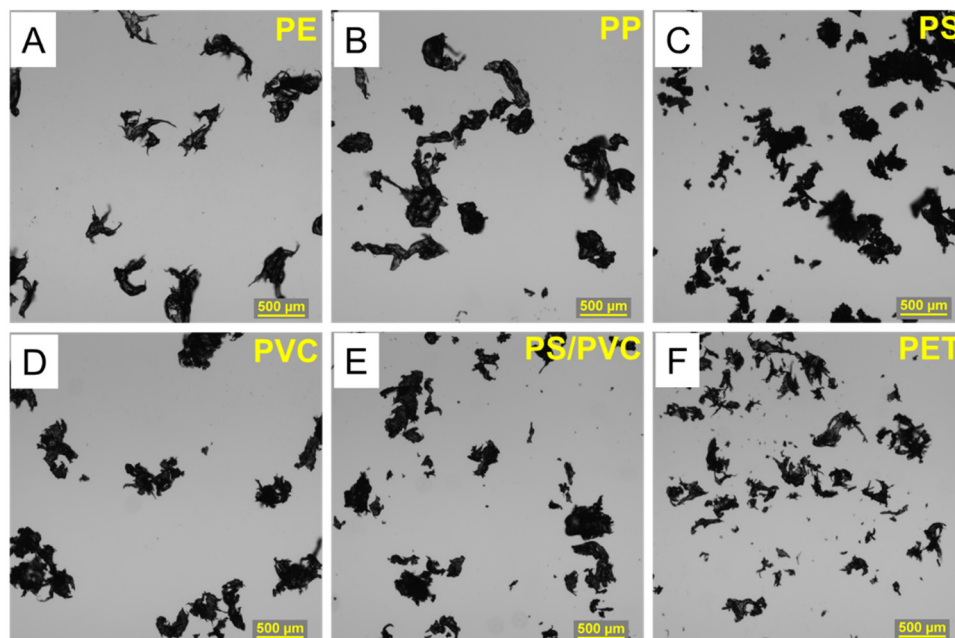


**Figure 2.** Micrographs of the microplastics acquired by shredding plastic materials composed of (A) PE, (B) PP, (C) PS, (D) PVC, (E) composite of PS/PVC, and (F) PET.

## Adsorption of Linear DNA onto Microplastics

At pH 7.6, the  $\zeta$ -potentials of the microplastics were all negative (Figure 3A), thereby repelling negatively charged DNA (Figure 3B). To screen the charge repulsion between the microplastics and DNA, different metal ions including  $\text{Na}^+$ ,  $\text{Mg}^{2+}$  or  $\text{Ca}^{2+}$  were added to the reaction buffer.<sup>41-43</sup> Environmental waters typically contain high concentrations of these metal ions (e.g.  $\sim 450$  mM  $\text{Na}^+$ , 50 mM  $\text{Mg}^{2+}$ , and 10 mM  $\text{Ca}^{2+}$  in seawater).<sup>44</sup>

First, adsorption of 10 nM of a carboxyfluorescein (FAM)-labeled 21-mer single-stranded DNA onto the microplastics was tested in the presence of 200 mM  $\text{Na}^+$ , 2 mM  $\text{Mg}^{2+}$ , or 2 mM  $\text{Ca}^{2+}$  (Figure 3C). None to negligible adsorption of the DNA occurred on PE, PP, PVC, and PS/PVC. On the other hand, the DNA was adsorbed onto PS and PET to different extents. Likely, the different chemical structure of the microplastics accounted for the different DNA adsorption efficiencies (compare the insets in Figure 1). The aromatic rings in PS and PET can provide  $\pi$ - $\pi$  stacking with DNA nucleobases, cation- $\pi$  interactions with the metal ions, and hydrogen bonding. Moreover, the carboxyl, hydroxyl and ester functional groups in PET could also enhance its interaction with DNA via hydrogen bonding, which could explain the higher efficiency of PET than PS. On the other hand, PE, PP and PVC did not have aromatic structures and thus they showed weaker interactions with DNA. Moreover, comparing the metal ions,  $\text{Mg}^{2+}$  and  $\text{Ca}^{2+}$  were more efficient than  $\text{Na}^+$  for promoting the adsorption. With 2 mM  $\text{Ca}^{2+}$ , 28% and 87% of the DNA was adsorbed on PS and PET, respectively (Figure 3C).

The effect of metal concentration on DNA adsorption on the PET and PS microplastics was then tested, and a higher adsorption efficiency onto PET was confirmed for all the metal ions (Figure 3D-F). The data fitted well with a one-site binding model, and thus the apparent metal dissociate constants ( $K_d$ ) were calculated. The efficiency of  $\text{Mg}^{2+}$  and  $\text{Ca}^{2+}$  to induce the DNA adsorption on PET was almost the same with a  $K_d$  of 66  $\mu\text{M}$  (Figure 3E,F). However, a  $\sim 85$ -fold higher concentration of  $\text{Na}^+$  was needed to reach the half-saturation ( $K_d$  of 5.7 mM). Similarly, the  $K_d$  of  $\text{Na}^+$ ,  $\text{Mg}^{2+}$ , and  $\text{Ca}^{2+}$  for promoting DNA adsorption on PS was calculated to be 49 mM, 0.87 mM, and 0.12 mM, respectively.  $\text{Mg}^{2+}$  and  $\text{Ca}^{2+}$  can bridge the DNA adsorption, which may explain their higher efficiency than  $\text{Na}^+$ .<sup>43, 45</sup> Similar metal-dependent adsorption were also reported with other surfaces such as polydopamine and graphene oxide.<sup>31, 45</sup>

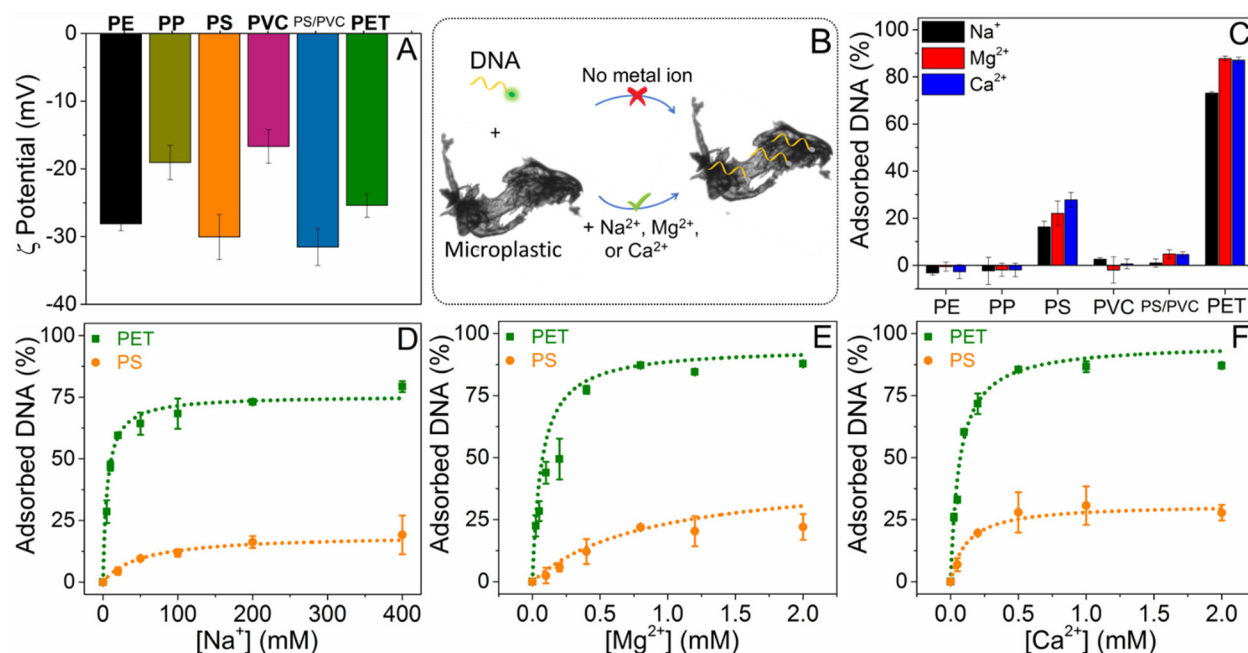


**Figure 3.** (A)  $\zeta$ -Potentials of different microplastics in 10 mM HEPES buffer, pH 7.6. (B) A scheme illustrating the effect of metal ions for promoting DNA adsorption on the PS and PET microplastics. (C) Adsorption of 10 nM FAM-DNA onto 50  $\mu\text{g}/\text{mL}$  of different microplastics in the presence of 200 mM Na<sup>+</sup>, 2 mM Mg<sup>2+</sup>, or 2 mM Ca<sup>2+</sup>. Adsorption of 10 nM FAM-DNA on 50  $\mu\text{g}/\text{mL}$  of the PET and PS microplastics in the presence of different concentrations of (D) Na<sup>+</sup>, (E) Mg<sup>2+</sup>, or (F) Ca<sup>2+</sup>.

### Adsorption of SNA onto Microplastics

After understanding the adsorption of linear DNA, we then tested the adsorption of SNA on the microplastics. The same DNA sequence bearing a 5'-SH was densely functionalized on 13 nm diameter AuNPs to form SNAs. The sequence DNA included a 9-adenine block, since it is a commonly used spacer for preparing SNA. On average 127 DNA strands were attached to each 13 nm AuNP, and the total DNA concentration was  $\sim 200$  nM for the adsorption experiments. Polyvalent binding of SNA can enhance individual weak interactions between DNA and nanomaterials, thereby leading to more stable adsorption.<sup>30-32</sup> This could provide us with more insights into the interactions between DNA and microplastics. Figure 4A is a TEM image depicting

the adsorbed SNA onto a PET microplastic particle in the presence of 4 mM  $Mg^{2+}$ , where the AuNPs were densely adsorbed.

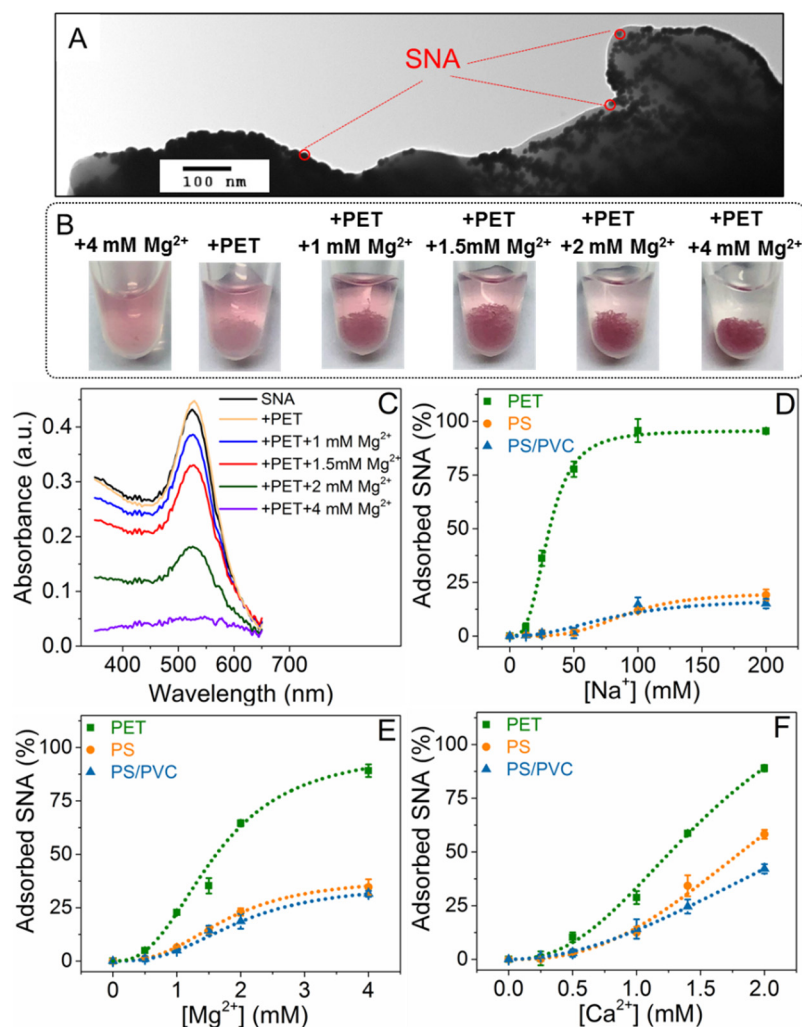


**Figure 4.** (A) A TEM micrograph depicting a high density of SNA adsorbed onto a PET microplastic in the presence of 4 mM  $Mg^{2+}$ . (B) Photographs illustrating the effect of  $Mg^{2+}$  concentration on the adsorption of 1.58 nM SNA (total of 200 nM DNA) onto  $\sim 150 \mu\text{g/mL}$  of the PET microplastics. (C) UV-vis spectra of the supernatants collected from the samples shown in panel (B). The adsorbed SNA was quantified according to the decrease of the absorbance. Adsorption of 1.58 nM SNA onto  $150 \mu\text{g/mL}$  of the PET, PS, and PS/PVC microplastics in the presence of different concentrations of (D)  $Na^+$ , (E)  $Mg^{2+}$ , or (F)  $Ca^{2+}$ .

The adsorption of the SNA was quantified according to the decrease of the AuNP absorbance in the supernatants (Figure 4B, C). First, SNA adsorption onto the six types of microplastics were measured in the presence of 200 mM Na<sup>+</sup>, 4 mM Mg<sup>2+</sup>, or 2 mM Ca<sup>2+</sup> (Figure S2). Similar to the linear DNA, the SNA was not adsorbed onto PE, PP, or PVC, while PET and PS microplastics showed the highest SNA adsorption efficiency. Interestingly, the microplastics of composite of PS/PVC could also adsorb the SNA, although it did not adsorb the linear DNA (Figure S2). This revealed the stronger polyvalent interactions enabled by the SNA. Note that the as-prepared citrate-capped AuNPs are aggregated by salt and thus we could not use salt to promote their adsorption (Figure S3).

We then studied the effect of metal concentration to induce SNA adsorption onto PET, PS, and PS/PVC. In this case, the shape of the binding curves was very different from the adsorption of the linear DNA in Figure 3. For SNA, sigmoidal binding curves were observed (Figure 4D-F), indicative of cooperative action of multiple metal ions for promoting SNA adsorption.<sup>31</sup> The data were fitted well with the Hill equation. From the apparent dissociation constant for different microplastics in the presence of the same metal ion, the SNA adsorption efficiency followed the order of PET, PS, and PS/PVC, which was the same order as for the adsorption of the linear DNA. The Hill coefficients were obtained for different metal ions and microplastics. Overall, for the same microplastic, the Hill coefficients for Na<sup>+</sup> (PET (3.2), PS (3.7), PS-PVC (2.7)) were higher than for Mg<sup>2+</sup> (PET (2.6), PS (2.8), PS/PVC (2.7)) and Ca<sup>2+</sup> (PET (2.4), PS (2.2), PS/PVC (2.0)). This suggested that more Na<sup>+</sup> ions than Mg<sup>2+</sup> or Ca<sup>2+</sup> were needed to achieve the cooperative binding effect of the SNA adsorption, which can be explained by their different charges.

### **DNA Desorption Studies**

The above studies investigated the efficiency of microplastics for DNA adsorption. The adsorption efficiency is influenced by not only the adsorption affinity but also the adsorption capacity. Therefore, to directly compare the adsorption affinity of microplastics, we also performed desorption studies by adding competing and denaturing agents to the pe-adsorbed DNA.

For the linear DNA, in the presence of 200 mM Na<sup>+</sup>, 2 mM Mg<sup>2+</sup>, or 2 mM Ca<sup>2+</sup>, a high adsorption can be achieved only on PET (Figure 3C), allowing us to perform desorption studies only on PET. For all the three metal ions, ~35% of the linear DNA was desorbed from PET by 4

M urea (Figure 5A). In a control experiment, adding water instead of competing agents induced negligible DNA desorption. Since urea can disrupt hydrogen bonding, this revealed the significant role of hydrogen bonding for such adsorption. Then, 10 mM EDTA was separately added to probe the effect of polyvalent metal ions, since EDTA can strongly bind to  $Mg^{2+}$  and  $Ca^{2+}$  with logarithmic stability constant of 8.8 and 10.6, respectively.<sup>46</sup> In the presence of  $Na^+$ , the adsorbed DNA was undisturbed by EDTA (Figure 5A, black bar). Since EDTA can decrease the concentration of polyvalent metal ions to nanomolar region, this data showed that  $Na^+$  alone can promote the DNA adsorption on PET. On the other hand, in the presence of  $Mg^{2+}$  and  $Ca^{2+}$ , 48% and 33% of the pre-adsorbed DNA strands were desorbed from PET after adding EDTA (Figure 5A, red and blue bar) showing the critical role of these divalent metal ions for the adsorption. Although EDTA has a higher stability constant for  $Ca^{2+}$ , less of the DNA was desorbed compared to the case of  $Mg^{2+}$ , suggesting that the DNA adsorption on PET was tighter in the presence of  $Ca^{2+}$  than  $Mg^{2+}$ . Therefore, the role of metal ions for DNA adsorption was confirmed.

Typically, adding phosphate or adenosine can probe the binding via phosphate backbone or nucleobases of DNA.<sup>47</sup> When 5 mM phosphate or 5 mM adenosine was added, negligible desorption occurred (Figure 5A), suggesting that neither the DNA phosphate nor nucleobases dominated in the adsorption mechanism, but rather they both contributed to the adsorption. Finally, a surfactant (0.25% Tween 80), was added to the pre-adsorbed DNA, and the DNA was almost completely desorbed regardless of the type of metal ion present. This suggested that the surfactant likely interacted with PET via its hydrophobic tail and using van der Waals (VDW) force to displace the DNA. Beside the mentioned interactions, microporous filling mechanisms may also contribute to the adsorption onto the microplastics,<sup>48</sup> where DNA might diffuse into the microplastics pores and be entrapped in there.

As mentioned above, linear DNA cannot be effectively adsorbed onto PS and PS/PVC unlike PET (Figure 3C). However, 200 nM SNA was thoroughly adsorbed in the presence of 4 mM  $Mg^{2+}$ , or 2 mM  $Ca^{2+}$  after overnight incubation (Figure 5B, C). This provided a chance of comparing the adsorption affinity of PET, PS, and PS/PVC *via* desorption studies. 4 M urea and 10 mM EDTA were separately added to the pre-adsorbed SNA on the microplastics. For PET, almost no desorption occurred with urea, and negligible desorption occurred with (Figure 5D, E). This suggests an extraordinary stability of SNA adsorption on PET, which was enhanced compared

to the linear DNA (compare to the urea- and EDTA-induced desorption in Figure 5A).<sup>30-31</sup> Desorption from PET was in all cases lower than PS, and PS/PVC (Figure 5D, E) suggesting that PET had the highest affinity for DNA among these microplastics. For PS, urea desorbed 80% and 43% of the SNA in the presence of  $Mg^{2+}$  and  $Ca^{2+}$ , respectively (Figure 5D), confirming that a tighter adsorption can be achieved with  $Ca^{2+}$ . For PS/PVC, the urea-induced adsorption was 25% and 15% in the presence of  $Mg^{2+}$  and  $Ca^{2+}$  (Figure 5D), which was interestingly lower than for PS. EDTA-induced desorption also confirmed a tighter binding with  $Ca^{2+}$  than  $Mg^{2+}$ , and a higher affinity of PS/PVC than PS (Figure 5E).

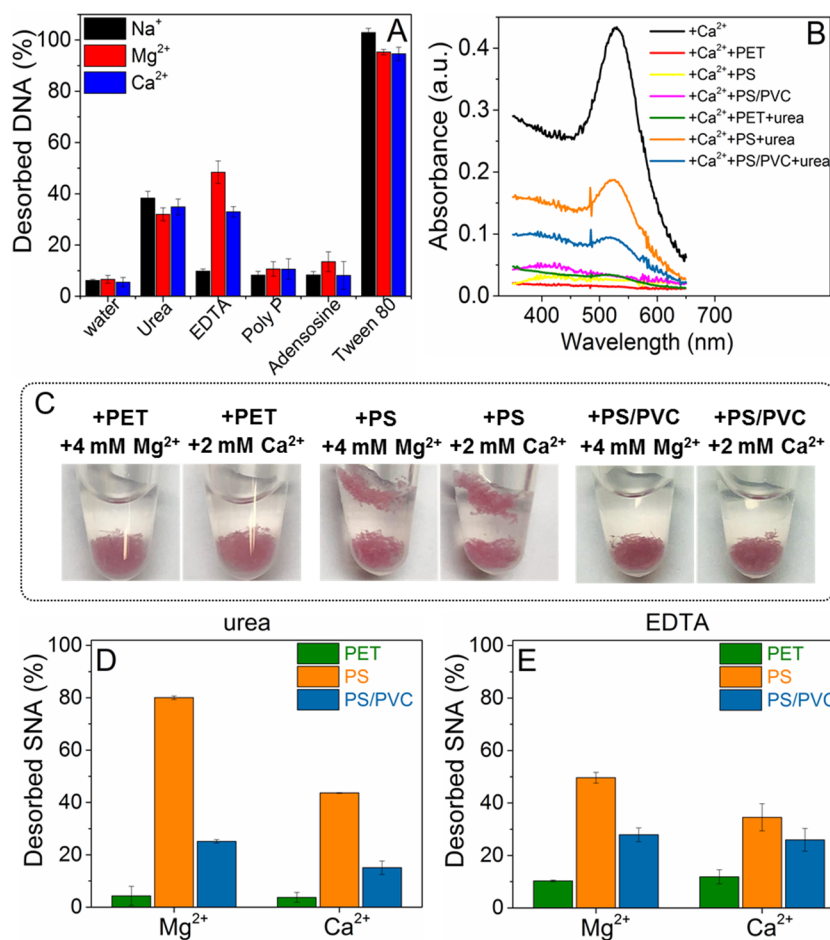


**Figure 5.** (A) The desorption of linear DNA from the PET microplastics in the presence of different metal ions (200 mM Na<sup>+</sup>, 2 mM Mg<sup>2+</sup>, or 2 mM Ca<sup>2+</sup>) induced by 4 M urea, 10 mM EDTA, 5 mM polyphosphate, 5 mM adenosine, or 0.25% Tween 80. (B) Photographs depicting the complete adsorption of 1.58 nM SNA on the PET, PS, and PS/PVC microplastics in the presence of 4 mM Mg<sup>2+</sup>, or 2 mM Ca<sup>2+</sup> after overnight incubation. (C) UV-vis spectra of the

supernatants collected from different samples demonstrating the urea-induced desorption of SNA from the PET, PS, and PS/PVC microplastics in the presence of 2 mM  $\text{Ca}^{2+}$ . The desorption of SNA from the PET, PS, and PS/PVC microplastics in the presence of different metal ions (200 mM  $\text{Na}^+$ , 4 mM  $\text{Mg}^{2+}$ , or 2 mM  $\text{Ca}^{2+}$ ) included by (D) 4 M urea, or (E) 10 mM EDTA.

Overall, the desorption data indicated the order of DNA adsorption affinity as following: PET>PS/PVC>PS. The composite of PS/PVC, besides all the attraction forces provided by PS, probably can harness some extra forces provided by PVC such as halogen bonding. The chlorine atoms in PVC structure can act as electron acceptors while the oxygen, nitrogen and the aromatic nucleobase of DNA are electron rich sites that may function as electron donor to form halogen bonds.<sup>49-50</sup>

## Conclusions

In summary, the interactions of DNA oligonucleotides with a few most common microplastic materials were investigated including PE, PP, PS, PVC, PS/PVC, and PET. Adsorption of linear DNA and SNA onto the microplastics were tested in the presence of  $\text{Na}^+$ ,  $\text{Mg}^{2+}$  or  $\text{Ca}^{2+}$  ions. The linear DNA adsorbed onto PET and PS more efficiently than the other microplastics, likely due to the aromatic functional groups present in the PET and PS structure. Desorption studies revealed that hydrogen bonding and metal-mediated interactions are the predominant forces between DNA and PET microplastics. However, VDW force and hydrophobic interactions are also likely involved in the adsorption mechanism. Unlike the linear DNA, stable adsorption of high concentrations of SNA were also achieved on PS and PS/PVC microplastics. Investigation of the SNA desorption from the microplastics suggested the order of adsorption affinity to be PET>PS/PVC >PS. Moreover, overall,  $\text{Ca}^{2+}$  and  $\text{Mg}^{2+}$  promoted a more efficient and a tighter DNA adsorption than  $\text{Na}^+$ . This study has provided interesting insights to better comprehend the origins of interactions between microplastics and environmental DNA. In addition, it has supplied fundamental information which paves the way toward the future application of DNA aptamers in microplastic studies.

## Acknowledgements

Funding for this work was from the Natural Sciences and Engineering Research Council of Canada (NSERC).

### Supporting Information

Characteristic Raman peaks attributed to different plastic materials, photographs of the microplastics after grating, adsorption efficiency of SNA onto different microplastics in the presence of different metal ions, and effect of metal ions on the stability of the bare AuNPs or SNA.

### Notes

The authors declare no competing financial interest.

### References

1. Geyer, R., Production, Use, and Fate of Synthetic Polymers. In *Plastic Waste and Recycling*, Elsevier: 2020; pp 13-32.
2. Chae, Y.; An, Y.-J., Current Research Trends on Plastic Pollution and Ecological Impacts on the Soil Ecosystem: A Review. *Environ. Pollut.* **2018**, *240*, 387-395.
3. Reid, A. J.; Carlson, A. K.; Creed, I. F.; Eliason, E. J.; Gell, P. A.; Johnson, P. T.; Kidd, K. A.; MacCormack, T. J.; Olden, J. D.; Ormerod, S. J., Emerging Threats and Persistent Conservation Challenges for Freshwater Biodiversity. *Biol. Rev.* **2019**, *94* (3), 849-873.
4. Prokić, M. D.; Radovanović, T. B.; Gavrić, J. P.; Faggio, C., Ecotoxicological Effects of Microplastics: Examination of Biomarkers, Current State and Future Perspectives. *TrAC, Trends Anal. Chem.* **2019**, *111*, 37-46.
5. Ivleva, N. P., Chemical Analysis of Microplastics and Nanoplastics: Challenges, Advanced Methods, and Perspectives. *Chem. Rev.* **2021**, *121* (19) 11886–11936.
6. Rech, S.; Borrell, Y.; García-Vazquez, E., Marine Litter as a Vector for Non-Native Species: What We Need to Know. *Mar. Pollut. Bull.* **2016**, *113* (1-2), 40-43.
7. de Oliveira, T. T. S.; Andreu, I.; Machado, M. C.; Vimbela, G.; Tripathi, A.; Bose, A., Interaction of Cyanobacteria with Nanometer and Micron Sized Polystyrene Particles in Marine and Fresh Water. *Langmuir* **2020**, *36* (14), 3963-3969.

8. Al Harraq, A.; Bharti, B., Microplastics through the Lens of Colloid Science. *ACS Environ. Au* **2021**, DOI: 10.1021/acsenvironau.1c00016.
9. Cox, K. D.; Covernton, G. A.; Davies, H. L.; Dower, J. F.; Juanes, F.; Dudas, S. E., Human Consumption of Microplastics. *Environ. Sci. Technol.* **2019**, *53* (12), 7068-7074.
10. Sharma, S.; Chatterjee, S., Microplastic Pollution, a Threat to Marine Ecosystem and Human Health: A Short Review. *Environ. Sci. Pollut. Res.* **2017**, *24* (27), 21530-21547.
11. Prata, J. C.; da Costa, J. P.; Lopes, I.; Duarte, A. C.; Rocha-Santos, T., Environmental Exposure to Microplastics: An Overview on Possible Human Health Effects. *Sci. Total Environ.* **2020**, *702*, 134455.
12. Koelmans, A. A.; Nor, N. H. M.; Hermsen, E.; Kooi, M.; Mintenig, S. M.; De France, J., Microplastics in Freshwaters and Drinking Water: Critical Review and Assessment of Data Quality. *Water Res.* **2019**, *155*, 410-422.
13. Liu, B.; Salgado, S.; Maheshwari, V.; Liu, J., DNA Adsorbed on Graphene and Graphene Oxide: Fundamental Interactions, Desorption and Applications. *Curr. Opin. Colloid Interface Sci.* **2016**, *26*, 41-49.
14. Lu, C.; Liu, Y.; Ying, Y.; Liu, J., Comparison of MoS<sub>2</sub>, WS<sub>2</sub>, and Graphene Oxide for DNA Adsorption and Sensing. *Langmuir* **2017**, *33* (2), 630-637.
15. Liu, B.; Zhao, Y.; Jia, Y.; Liu, J., Heating Drives DNA to Hydrophobic Regions While Freezing Drives DNA to Hydrophilic Regions of Graphene Oxide for Highly Robust Biosensors. *J. Am. Chem. Soc.* **2020**, *142* (34), 14702-14709.
16. Zandieh, M.; Liu, J., Transition Metal-Mediated DNA Adsorption on Polydopamine Nanoparticles. *Langmuir* **2020**, *36* (12), 3260-3267.
17. Zandieh, M.; Liu, J., Metal-Doped Polydopamine Nanoparticles for Highly Robust and Efficient DNA Adsorption and Sensing. *Langmuir* **2021**, *37* (30), 8953-8960.
18. McCormick, A.; Hoellein, T. J.; Mason, S. A.; Schluep, J.; Kelly, J. J., Microplastic Is an Abundant and Distinct Microbial Habitat in an Urban River. *Environ. Sci. Technol.* **2014**, *48* (20), 11863-11871.
19. Debeljak, P.; Pinto, M.; Proietti, M.; Reisser, J.; Ferrari, F. F.; Abbas, B.; Van Loosdrecht, M. C.; Slat, B.; Herndl, G. J., Extracting DNA from Ocean Microplastics: A Method Comparison Study. *Anal. Methods* **2017**, *9* (9), 1521-1526.

20. Jiang, P.; Zhao, S.; Zhu, L.; Li, D., Microplastic-Associated Bacterial Assemblages in the Intertidal Zone of the Yangtze Estuary. *Sci. Total Environ.* **2018**, *624*, 48-54.
21. Ibabe, A.; Rayon, F.; Martinez, J. L.; Garcia-Vazquez, E., Environmental DNA from Plastic and Textile Marine Litter Detects Exotic and Nuisance Species Nearby Ports. *PLoS one* **2020**, *15* (6), e0228811.
22. Gaillard, C.; Strauss, F., Avoiding Adsorption of DNA to Polypropylene Tubes and Denaturation of Short DNA Fragments. *Tech. Tips Online* **1998**, *3* (1), 63-65.
23. Klein, D.; Gurevich, L.; Janssen, J.; Kouwenhoven, L.; Carbeck, J.; Sohn, L., Ordered Stretching of Single Molecules of Deoxyribose Nucleic Acid between Microfabricated Polystyrene Lines. *Appl. Phys. Lett.* **2001**, *78* (16), 2396-2398.
24. Benke, A.; Mertig, M.; Pompe, W., Ph-and Salt-Dependent Molecular Combing of DNA: Experiments and Phenomenological Model. *Nanotechnology* **2010**, *22* (3), 035304.
25. Zhou, Y.; Huang, Z.; Yang, R.; Liu, J., Selection and Screening of DNA Aptamers for Inorganic Nanomaterials. *Chem. Eur. J.* **2018**, *24* (11), 2525-2532.
26. Cutler, J. I.; Auyeung, E.; Mirkin, C. A., Spherical Nucleic Acids. *J. Am. Chem. Soc.* **2012**, *134* (3), 1376-1391.
27. Banga, R. J.; Chernyak, N.; Narayan, S. P.; Nguyen, S. T.; Mirkin, C. A., Liposomal Spherical Nucleic Acids. *J. Am. Chem. Soc.* **2014**, *136* (28), 9866-9869.
28. Liu, B.; Liu, J., Interface-Driven Hybrid Materials Based on DNA-Functionalized Gold Nanoparticles. *Matter* **2019**, *1* (4), 825-847.
29. Hao, Y.; Li, Y.; Song, L.; Deng, Z., Flash Synthesis of Spherical Nucleic Acids with Record DNA Density. *J. Am. Chem. Soc.* **2021**, *143* (8), 3065-3069.
30. Liu, B.; Huang, Z.; Liu, J., Polyvalent Spherical Nucleic Acids for Universal Display of Functional DNA with Ultrahigh Stability. *Angew. Chem. Int. Ed.* **2018**, *57* (30), 9439-9442.
31. Zandieh, M.; Liu, J., Cooperative Metal Ion-Mediated Adsorption of Spherical Nucleic Acids with a Large Hysteresis. *Langmuir* **2020**, *36* (47), 14324-14332.
32. Zandieh, M.; Liu, J., Spherical Nucleic Acid Mediated Functionalization of Polydopamine-Coated Nanoparticles for Selective DNA Extraction and Detection. *Bioconjugate Chem.* **2021**, *32* (4), 801-809.

33. Fong, L.-K.; Wang, Z.; Schatz, G. C.; Luijten, E.; Mirkin, C. A., The Role of Structural Enthalpy in Spherical Nucleic Acid Hybridization. *J. Am. Chem. Soc.* **2018**, *140* (20), 6226-6230.
34. Bretti, C.; Cardiano, P.; Irto, A.; Lando, G.; Milea, D.; Sammartano, S., Interaction of N-Acetyl-L-Cysteine with Na<sup>+</sup>, Ca<sup>2+</sup>, Mg<sup>2+</sup> and Zn<sup>2+</sup>. Thermodynamic Aspects, Chemical Speciation and Sequestering Ability in Natural Fluids. *J. Mol. Liq.* **2020**, *319*, 114164.
35. Liu, J.; Lu, Y., Preparation of Aptamer-Linked Gold Nanoparticle Purple Aggregates for Colorimetric Sensing of Analytes. *Nat. Protoc.* **2006**, *1* (1), 246-252.
36. Araujo, C. F.; Nolasco, M. M.; Ribeiro, A. M.; Ribeiro-Claro, P. J., Identification of Microplastics Using Raman Spectroscopy: Latest Developments and Future Prospects. *Water Res.* **2018**, *142*, 426-440.
37. Sobhani, Z.; Al Amin, M.; Naidu, R.; Megharaj, M.; Fang, C., Identification and Visualisation of Microplastics by Raman Mapping. *Anal. Chim. Acta* **2019**, *1077*, 191-199.
38. Liu, B.; Liu, J., Freezing Directed Construction of Bio/Nano Interfaces: Reagentless Conjugation, Denser Spherical Nucleic Acids, and Better Nanoflares. *J. Am. Chem. Soc.* **2017**, *139* (28), 9471-9474.
39. Gillibert, R.; Balakrishnan, G.; Deshoules, Q.; Tardivel, M.; Magazzù, A.; Donato, M. G.; Maragò, O. M.; Lamy de La Chapelle, M.; Colas, F.; Lagarde, F., Raman Tweezers for Small Microplastics and Nanoplastics Identification in Seawater. *Environ. Sci. Technol.* **2019**, *53* (15), 9003-9013.
40. de Ruijter, V. N.; Redondo-Hasselerharm, P. E.; Gouin, T.; Koelmans, A. A., Quality Criteria for Microplastic Effect Studies in the Context of Risk Assessment: A Critical Review. *Environ. Sci. Technol.* **2020**, *54* (19), 11692-11705.
41. Kushalkar, M. P.; Liu, B.; Liu, J., Promoting DNA Adsorption by Acids and Polyvalent Cations: Beyond Charge Screening. *Langmuir* **2020**, *36* (38), 11183-11195.
42. Wu, X.; Liu, P.; Huang, H.; Gao, S., Adsorption of Triclosan onto Different Aged Polypropylene Microplastics: Critical Effect of Cations. *Sci. Total Environ.* **2020**, *717*, 137033.
43. Xiong, Y.; Zhao, J.; Li, L.; Wang, Y.; Dai, X.; Yu, F.; Ma, J., Interfacial Interaction between Micro/Nanoplastics and Typical Ppcps and Nanoplastics Removal Via Electrosorption from an Aqueous Solution. *Water Res.* **2020**, *184*, 116100.

43. Besson, P.; Degboe, J.; Berge, B.; Chavagnac, V.; Fabre, S.; Berger, G., Calcium, Na, K and Mg Concentrations in Seawater by Inductively Coupled Plasma-Atomic Emission Spectrometry: Applications to Iapso Seawater Reference Material, Hydrothermal Fluids and Synthetic Seawater Solutions. *Geostand. Geoanalytical Res.* **2014**, *38* (3), 355-362.
45. Meng, Y.; Liu, P.; Zhou, W.; Ding, J.; Liu, J., Bioorthogonal DNA Adsorption on Polydopamine Nanoparticles Mediated by Metal Coordination for Highly Robust Sensing in Serum and Living Cells. *ACS Nano* **2018**, *12* (9), 9070-9080.
46. Anderegg, G., *Critical Survey of Stability Constants of Edta Complexes: Critical Evaluation of Equilibrium Constants in Solution: Stability Constants of Metal Complexes.* Elsevier: 2013.
47. Liu, B.; Ma, L.; Huang, Z.; Hu, H.; Wu, P.; Liu, J., Janus DNA Orthogonal Adsorption of Graphene Oxide and Metal Oxide Nanoparticles Enabling Stable Sensing in Serum. *Mater. Horiz.* **2018**, *5* (1), 65-69.
48. Wang, Y.; Yang, Y.; Liu, X.; Zhao, J.; Liu, R.; Xing, B., Interaction of Microplastics with Antibiotics in Aquatic Environment: Distribution, Adsorption, and Toxicity. *Environ. Sci. Technol.* **2021**, *5* (23), 15579–15595.
49. Parisini, E.; Metrangolo, P.; Pilati, T.; Resnati, G.; Terraneo, G., Halogen Bonding in Halocarbon–Protein Complexes: A Structural Survey. *Chem. Soc. Rev.* **2011**, *40* (5), 2267-2278.
50. Jimmy Huang, P.-J.; Moon, W. J.; Liu, J., Instantaneous Iodine-Assisted Dnazyme Cleavage of Phosphorothioate RNA. *Biochem.* **2018**, *58* (5), 422-429.

### For TOC Graphics Only

